

Compressed Sensing Signal Recovery via Forward-Backward Pursuit

Nazim Burak Karahanoglu^{a,b,*}, Hakan Erdogan^a

^aDepartment of Electronics Engineering, Sabanci University, Istanbul 34956, Turkey

^bInformation Technologies Institute, TUBITAK-BILGEM, Kocaeli 41470, Turkey

Abstract

Recovery of sparse signals from compressed measurements constitutes an ℓ_0 norm minimization problem, which is unpractical to solve. A number of sparse recovery approaches have appeared in the literature, including ℓ_1 minimization techniques, greedy pursuit algorithms, Bayesian methods and nonconvex optimization techniques among others. This manuscript introduces a novel two-stage greedy approach, called the Forward-Backward Pursuit (FBP). FBP is an iterative approach where each iteration consists of consecutive forward and backward stages. The forward step first expands the support estimate by the forward step size, while the following backward step shrinks it by the backward step size. The forward step size is higher than the backward step size, hence the initially empty support estimate is expanded at the end of each iteration. Forward and backward steps are iterated until the residual power of the observation vector falls below a threshold. This structure of FBP does not necessitate the sparsity level to be known *a priori* in contrast to the Subspace Pursuit or Compressive Sampling Matching Pursuit algorithms. FBP recovery performance is demonstrated via simulations including recovery of random sparse signals with different nonzero coefficient distributions in noisy and noise-free scenarios in addition to the recovery of a sparse image.

Keywords: compressed sensing, forward-backward search, sparse signal reconstruction, greedy algorithms, two-stage thresholding

1. Introduction

Despite the conventional acquisition process which captures a signal as a whole prior to dimensionality reduction via transform coding, Compressed Sensing (CS) aims at acquisition of sparse or compressible signals directly in reduced dimensions. Mathematically, the "compressed" observations are obtained via an observation matrix Φ

$$\mathbf{y} = \Phi \mathbf{x}, \quad (1)$$

where \mathbf{x} is a K -sparse signal of length N , K is the number of nonzero elements in \mathbf{x} , \mathbf{y} is the observation vector of length N and Φ is a $M \times N$ random matrix with $K < M < N$. Once \mathbf{y} is observed, the CS is to recover \mathbf{x} , which is analytically ill-posed following the dimensionality reduction via Φ . Exploiting the sparse nature of \mathbf{x} , CS reformulates (1) as a sparsity-promoting optimization problem

$$\mathbf{x} = \arg \min \|\mathbf{x}\|_0 \quad s.t. \quad \mathbf{y} = \Phi \mathbf{x}, \quad (2)$$

where $\|\mathbf{x}\|_0$, called the ℓ_0 norm by abuse of terminology, denotes the number of nonzero elements in \mathbf{x} . As direct solution of (2) is computationally intractable, a number of alternative and approximate solutions have emerged in the literature. An overview of mainstream methods is available in [1], which

broadly categorizes CS algorithms as convex relaxation techniques, greedy pursuits, Bayesian methods and nonconvex optimization techniques. Theoretical exact recovery guarantees have also been developed mainly under the Restricted Isometry Property (RIP) [2, 3, 4] for some of the algorithms. RIP also provides a basis for understanding what type of observation matrices should be employed. Random matrices with Gaussian or Bernoulli entries, or matrices randomly selected from the discrete Fourier transform satisfy RIP with high probabilities.

Convex relaxation methods [2, 5, 6, 7, 8, 9] replace the ℓ_0 minimization in (2) with its closest convex approximation, the ℓ_1 minimization. Following this modification, recovery is tractable via convex optimization algorithms such as linear programming, as proposed by Basis Pursuit (BP) [8], which is historically the first convex relaxation algorithm. Greedy pursuit algorithms, such as Matching Pursuit (MP) [10], Orthogonal MP (OMP) [11], Compressive Sampling MP (CoSaMP) [12], Subspace Pursuit (SP) [13] and Iterative Hard Thresholding (IHT) [14, 15], employ iterative mechanisms. Among these, MP and OMP build up the support of \mathbf{x} iteratively, adding one element per iteration. SP and CoSaMP, on the other hand, apply a two-stage iterative scheme, which at each iteration first expands and then shrinks the support by the same number of elements, keeping the support size fixed between iterations. IHT combines gradient descent with a thresholding step. [16] provides an algorithmic framework called Two-Stage Thresholding (TST), into which algorithms such as SP, CoSaMP and IHT fall.

The manuscript at hand proposes a two-stage iterative greedy algorithm, called the Forward-Backward Pursuit (FBP). As the

*Corresponding author

Email addresses: karahanoglu@sabanciuniv.edu (Nazim Burak Karahanoglu), haerdogan@sabanciuniv.edu (Hakan Erdogan)

name indicates, FBP employs forward selection and backward removal steps which iteratively expand and shrink the support estimate of \mathbf{x} . Though this structure is close to SP or CoSaMP, FBP has a major difference from these: Forward and backward step sizes of FBP are not the same. Forward step size is higher than the backward step size, hence the support estimate is iteratively expanded. With this structure, FBP falls into the general category of TST-type algorithms, while iterative expansion of the support estimate is investigated for the first time in this concept. The recovery abilities of FBP are demonstrated on sparse signals with different nonzero coefficient distributions in noiseless and noisy observation scenarios, and on a sparse image in comparison to BP, SP and OMP. These results indicate that FBP can perform better than SP and BP in most scenarios, which indicates that SP is not necessarily the globally optimum TST scheme as proposed in [16]. A preliminary version of this work has been presented at EUSIPCO'2012.

Its two-stage structure with different forward and backward step sizes gives FBP some advantages over both SP and OMP. SP requires *a priori* estimate of the sparsity level, K , which is most of the time not available in practice. On the other hand, FBP expands the support estimate from scratch until the residual error of the observation is small enough (or vanishes for the noiseless case). Hence, FBP does not require K *a priori* in contrast to SP and CoSaMP. Additionally, the backward step of FBP can remove some possibly misplaced atoms from the support estimate of the support, which is an advantage over forward greedy algorithms such as OMP.

A forward-backward greedy approach for the sparse learning problem, FoBa, has been investigated in [17]. Though both FoBa and FBP consist of iterative forward and backward steps, the algorithms have some fundamental differences: The FoBa algorithm employs strict forward and backward step sizes of 1, while the forward and backward step sizes of FBP are typically greater than 1. As a result of the larger step sizes (actually the difference between forward and backward step sizes), FBP terminates in less iterations. In addition, FoBa takes the backward step after a few forward steps based on an adaptive decision. FBP employs no adaptive criterion for taking the backward step (note that this is not trivial when the backward step size is greater than 1). Finally, FoBa has been applied for the sparse learning problem, while we propose and evaluate FBP for sparse signal recovery from compressed measurements.

This manuscript is organized as follows: First, we give a brief overview of greedy pursuit algorithms. The FBP algorithm is introduced in Section 3. Section 4 is devoted to the demonstration of FBP recovery performance in comparison to the BP, SP and OMP algorithms. We conclude with a brief summary of our findings in Section 5.

2. Greedy Pursuits

In this section we summarize OMP, SP and TST, which are important for our purposes because of their resemblance to the FBP algorithm. Beforehand, we define the notation that is used throughout the paper: Let $S^{(k)}$ be the estimated support of \mathbf{x}

after the k th iteration, while $\tilde{S}^{(k)}$ stands for the expanded support after the forward selection step of the k th iteration. $\tilde{\mathbf{y}}^{(k)}$ denotes the approximation of \mathbf{y} after the k th iteration and $\mathbf{r}^{(k)}$ is the residue of \mathbf{y} after the k th iteration. Φ_S is the matrix composed of the columns of Φ indexed by S . Similarly, \mathbf{x}_S is the vector consisting of the entries of \mathbf{x} with indices in S .

OMP is a forward greedy algorithm that searches for the support of \mathbf{x} by identifying one element per iteration. It starts with an empty support estimate: $S^{(0)} = \emptyset$ and $\mathbf{r}^{(0)} = \mathbf{y}$. At the iteration k , OMP expands $S^{(k-1)}$, the support estimate of the previous iteration, with the index of the dictionary atom closest to $\mathbf{r}^{(k-1)}$, the residue of the last iteration (i.e. it selects the index of the largest magnitude entry of $\Phi^T \mathbf{r}^{(k-1)}$). Following this, $\tilde{\mathbf{y}}^{(k)}$ is computed via orthogonal projection of \mathbf{y} onto $\Phi_{S^{(k)}}$ and the residue is updated as $\mathbf{r}^{(k)} = \mathbf{y} - \tilde{\mathbf{y}}^{(k)}$. The iterations are carried out until the termination criterion is met.

In this work, we stop OMP when $\|\mathbf{r}^{(k)}\|_2$ falls below the threshold $\varepsilon\|\mathbf{y}\|_2$. A similar termination criterion is also defined in the next section for FBP. Another termination criterion commonly used for OMP is to run it for exactly K steps. Though, the choice for the termination criterion is mostly underestimated in literature, recent work of the authors [18] indicates that running for exactly K steps is suboptimal. Moreover, specifying K in practice is most of the time not trivial. On the other hand, termination based on the residual power of the observed vector indeed resembles the actual aim of exactly representing the observation, and improves the recovery of OMP-type algorithms as the recovery results in [18] suggest. As a result of employing the residue-based termination criterion, OMP recovery results in this work are comparable to, and for some cases even better than BP and SP. [18] provides a comparison of the two termination criterion for OMP-type algorithms. In the light of these results, the authors feel that the more optimal way of running OMP should involve a residue-based termination criterion.

SP and CoSaMP combine selection of multiple columns per iteration with a pruning step, maintaining K element support sets throughout the iterations. At iteration k , SP first expands the selected support with indices of the K largest magnitude entries of $\Phi^T \mathbf{r}^{(k-1)}$, obtaining an extended support $\tilde{S}^{(k)}$ of size $2K$ (Alternatively, CoSaMP expands the support by $2K$ elements.). In the second step, the orthogonal projection coefficients of \mathbf{y} onto $\Phi_{\tilde{S}^{(k)}}$ are computed, and the estimated support $S^{(k)}$ is obtained by pruning $\tilde{S}^{(k)}$ to contain only the indices of the K largest magnitude projection coefficients. $\mathbf{r}^{(k)}$ is finally computed using the approximation $\tilde{\mathbf{y}}^{(k)}$ which is obtained by orthogonal projection of \mathbf{y} onto $\Phi_{S^{(k)}}$. The iterations are stopped when $\|\mathbf{r}^{(k)}\|_2 \geq \|\mathbf{r}^{(k-1)}\|_2$. Once stopped at iteration l , the final estimate of the support is $S^{(l-1)}$, while orthogonal projection of \mathbf{y} onto $\Phi_{S^{(l-1)}}$ yields the corresponding nonzero values. CoSaMP and SP are provided with RIP-based theoretical guarantees, showing that these two-stage schemes reduce the reconstruction error iteratively when some certain RIP conditions are met.

Recently, Maleki and Donoho have presented an algorithmic framework called Two-Stage Thresholding (TST) [16], into which algorithms such as SP and CoSaMP fall. As the name suggests, this framework employs a two-stage iterative scheme. The first stage is similar to iterative thresholding algorithms: It

first updates the sparse estimate in the direction of $\Phi^T \mathbf{r}^{(k-1)}$ and then thresholds the result to get a new support estimate. The optimal coefficients are computed by orthogonal projection of \mathbf{y} onto the selected support. A second thresholding operator on these optimal coefficients yields the sparse estimate of the corresponding iteration. The evaluation of TST iterative thresholding algorithms in [16] announces an optimum TST version, which finally turns out to be the SP algorithm. Following this result, we involve SP in our simulations as a representative of TST schemes. Our results below also support the conclusion in [16] that SP is the best TST scheme for sparse signals with constant amplitudes, and hence it is the best worst-case performer. In addition, our results also show that SP is not globally the best TST algorithm, as FBP outperforms SP for some other distributions.

3. Forward-Backward Pursuit

Forward greedy algorithms, such as OMP and other MP variants, enlarge the support estimate iteratively via forward selection steps. In such schemes, any element that is inserted into the support cannot be removed. That an incorrect element remains in the support until termination may cause the recovery to fail. To illustrate, consider a well-known example: Let \mathbf{x} be the summation of two equal magnitude sinusoids with very close frequencies, f_1 and f_2 , and Φ be an overcomplete sinusoidal dictionary, containing atoms with frequencies f_1 , f_2 and $f_3 = (f_1 + f_2)/2$ among others. The first iteration of OMP selects the component with frequency f_3 . Then, during the next iterations, the algorithm tries to cover for this error by choosing components other than the two correct ones and fails.

SP and CoSaMP, on the other hand, are two-stage algorithms, which are based on iterative expansion and shrinkage of the support. This allows both addition and removal of nonzero indices to the support estimate. However, the support size of these algorithms is fixed between iterations, and they require an estimate of the sparsity level K *a priori*. This is an important handicap in most practical cases, where K is unknown or it is not desired to fix it. In [16], Maleki and Donoho propose a tuned SP algorithm, where they suggest a fixed support size for a given $\{M, N\}$ pair. In this approach, the support size is tuned based on the sparsity ratio K/M corresponding to the 50% exact recovery rate for the related M/N value. This motivation behind this choice is to select the support size as large as the sparsity level SP can exactly recover. As the optimum K/M rates are pre-computed, support size can be decided once M and N are provided. This tuned SP algorithm turns out to be optimal TST scheme according to the results in [16]. However, these results also indicate that choosing the support size of SP larger than the actual sparsity level degrades the recovery performance. Hence, though this tuned SP may be the optimum practical SP algorithm, its performance is still worse than that of the SP version that incorporates the actual sparsity level.

The Forward-Backward Pursuit algorithm provides an iterative two-stage scheme in which no *a priori* estimate of the sparsity level K is required. The first stage of FBP is the forward step which expands the support estimate by α atoms, where we

Algorithm 1 FORWARD-BACKWARD PURSUIT

```

Input:  $\Phi, \mathbf{y}$ 
Define:  $\alpha, \beta, K_{\max}, \varepsilon$ 
Initialize:  $S^{(0)} = \emptyset, \mathbf{r}^{(0)} = \mathbf{y}$ 
 $k = 0$ 
while true do
     $k = k + 1$ 
     $T_f = \{\text{indices corresponding to } \alpha \text{ largest magnitude elements in } \Phi^T \mathbf{r}^{(k-1)}\}$ 
     $\tilde{S}^{(k)} = S^{(k-1)} \cup T_f$ 
     $\tilde{\mathbf{w}} = \arg \min_{\mathbf{z}} \|\mathbf{y} - \Phi_{\tilde{S}^{(k)}} \mathbf{z}\|_2$ 
     $T_b = \{\text{indices corresponding to } \beta \text{ smallest magnitude elements in } \tilde{\mathbf{w}}\}$ 
     $S^{(k)} = \tilde{S}^{(k)} \setminus T_b$ 
     $\mathbf{w} = \arg \min_{\mathbf{z}} \|\mathbf{y} - \Phi_{S^{(k)}} \mathbf{z}\|_2$ 
     $\mathbf{r}^{(k)} = \mathbf{y} - \Phi_{S^{(k)}} \mathbf{w}$ 
    if  $\|\mathbf{r}^{(k)}\|_2 \leq \varepsilon \|\mathbf{y}\|_2$  or  $|S^{(k)}| \geq K_{\max}$  then
        break
    end if
end while
 $\tilde{\mathbf{x}}_{S^{(k)}} = \mathbf{w}$ 
 $\tilde{\mathbf{x}}_{\{1,2,\dots,N\} \setminus S^{(k)}} = 0$ 
return  $\tilde{\mathbf{x}}$ 

```

call α the forward step size. The second stage, then removes β atoms from the support. Similar to α , β is referred to as the backward step size. The forward step size is chosen larger than the backward step size, hence the support estimate is enlarged by $\alpha - \beta$ atoms at each iteration. The forward and backward steps are iterated until the residual power of the observation vector either vanishes or is less than a threshold value, which is proportional to the real power of the observation vector.

The FBP algorithm can be outlined as follows: We initialize the support estimate as an empty set: $S^{(0)} = \emptyset$, and the residue as $\mathbf{r}^{(0)} = \mathbf{y}$. At iteration k , first the forward step expands $S^{(k-1)}$ by indices of α largest magnitude elements in $\Phi^T \mathbf{r}^{(k-1)}$. This builds up the extended support $\tilde{S}^{(k)}$. Then the projection coefficients are computed by orthogonal projection of \mathbf{y} onto $\Phi_{\tilde{S}^{(k)}}$. The backward step prunes $\tilde{S}^{(k)}$ by removing the indices of β smallest magnitude projection coefficients, which produces the support estimate $S^{(k)}$. Finally, $\tilde{\mathbf{y}}^{(k)}$ is computed via orthogonal projection of \mathbf{y} onto $\Phi_{S^{(k)}}$ and the residue is updated as $\mathbf{r}^{(k)} = \mathbf{y} - \tilde{\mathbf{y}}^{(k)}$. The iterations are carried on until either $\|\mathbf{r}^{(k)}\|_2$ vanishes or falls below the threshold $\varepsilon \|\mathbf{y}\|_2$. In practice, we choose ε very small (on the order of 10^{-6} for the experiments in this paper) when the observations are noise-free. For noisy observations, ε should be selected depending on the noise level. To avoid the algorithm running for too many iterations in case of a failure, the maximum number of iterations is set as K_{\max} . After termination at iteration l , $S^{(l)}$ gives the nonzero indices of the estimate $\tilde{\mathbf{x}}$, and the corresponding nonzero elements are the projection coefficients of \mathbf{y} onto $S^{(l)}$. The pseudo-code of FBP is given in Algorithm 1.

Unlike the subspace methods SP and CoSaMP, FBP does not require an *a priori* estimate of the sparsity level K . As ex-

plained above, FBP enlarges the support estimate by $\alpha - \beta$ at each iteration until termination of the algorithm which is based on the residual power instead of the sparsity level. Hence, neither the backward step nor the termination criterion require an estimate of the sparsity level K . This, however, comes at a cost: The theoretical guarantees cannot be provided in a way similar to SP or CoSaMP, which make use of the support size being fixed as K after the backward step. For the time being, we cannot provide a complete theoretical analysis of FBP, and leave this as a future work. Note that, however, most of the theoretical analysis steps of SP or CoSaMP also hold for FBP.

Finally, let's go back to the example with the three sinusoids in order to demonstrate the advantages of using FBP instead of OMP. Remember that OMP fails for this example. Instead, assume we run FBP with $\alpha = 3$ and $\beta = 1$. During the forward step of the first iteration, FBP selects all the three components with frequencies f_1 , f_2 and f_3 . Following orthogonal projection, the backward step will eliminate f_3 , and the recovery will be successful after the first iteration.

4. Experimental Evaluation

This section is reserved for demonstration of the FBP recovery performance in comparison to BP, SP, OMP. For this purpose, we run recovery simulations involving different nonzero coefficient distributions, noiseless and noisy observations, and a sparse image. First, we compare exact recovery rates, average recovery error and run times of FBP with those of OMP, SP and BP for signals with nonzero elements drawn from the Gaussian distribution. In order to generalize the results to a wide range of M and K , we provide the empirical phase transition curves, which are obtained using the procedure in [16], for different distributions. Meanwhile, phase transition curves also serve for the purpose of investigating optimal α and β choices. We then demonstrate recovery from noisy observations, and finally test our proposal on an image to illustrate the recovery performance on a realistic coefficient distribution.

4.1. Exact Recovery Rates and Reconstruction Error

First, we compare the exact recovery rates, recovery error and run times of FBP using various α and β values with those of OMP, SP and BP. In these simulations, the signal and observation sizes are fixed as $N = 256$ and $M = 100$, while K varies in [10, 45]. For each K , recovery simulations are repeated over 500 randomly generated samples where the nonzero entries are drawn from the standard Gaussian distribution. From now on, we call this type of sparse signals the Gaussian sparse signals. For each test signal, a different observation matrix is drawn from the Gaussian distribution with mean 0 and standard deviation $1/N$. ε is set to 9×10^{-7} and K_{\max} is 55. Note that, ε and K_{\max} are also valid for OMP as OMP is also run until $\|\mathbf{r}\|_2 \leq \varepsilon \|\mathbf{y}\|_2$, with a maximum of K_{\max} iterations allowed. The recovery error is expressed in terms of Average Normalized Mean-Squared-Error (ANMSE), which is defined as

$$ANMSE = \frac{1}{500} \sum_{i=1}^{500} \frac{\|\mathbf{x}_i - \hat{\mathbf{x}}_i\|_2^2}{\|\mathbf{x}_i\|_2^2} \quad (3)$$

where $\hat{\mathbf{x}}_i$ is the recovery of the i th test vector \mathbf{x}_i .

Fig. 1 and 2 depict the reconstruction performance of FBP with various $\alpha - \beta$ choices for the Gaussian sparse signals in comparison to OMP, BP and SP. Fig. 1 is obtained by varying α in [2, 30], while $\beta = \alpha - 1$. That is, the forward step size varies, while the support estimate is expanded by one element per iteration. For Fig. 2, α is selected as 20, and β is varied in [13, 19], changing the increment in the support size per iteration for a fixed forward step size. The speeds of the FBP, SP and OMP algorithms are also compared, while BP is excluded as it is incomparably slower than the other algorithms. Roughly, these recovery results indicate that FBP shows better recovery than the other candidates in this example.

According to Fig. 1, increasing α while keeping the support increment, i.e. $\alpha - \beta$, fixed improves the recovery performance of FBP. We observe that the exact recovery rate of FBP is significantly better than the other candidates. BP, SP and OMP start to fail at around $K = 25$, while, for $\alpha \geq 20$, the FBP failures begin only when $K > 30$. As for the ANMSE, FBP is the best performer when $\alpha \geq 20$. With this setting, BP can beat FBP in ANMSE only when $K = 45$.

In Fig. 2, we observe that increasing β for a fixed α also improves the recovery performance. In this case, exact recovery rates significantly increase with the backward step size, while the ANMSE values remain mostly unaltered. This indicates that when β is increased, nonzero elements with smaller magnitudes, which do not significantly change the recovery error, can be better recovered. In comparison to the other algorithms involved in the simulation, FBP is the best performer for $\beta > 15$. As for the previous figure, BP can produce lower ANMSE than FBP only for $K = 45$.

As for the run times, we expectedly observe that increasing α or β slows down FBP, as these increase the dimensions of the orthogonal projection operations after the forward or backward steps. On the other hand, increasing $\alpha - \beta$ decreases the number of necessary iterations. As a result, FBP terminates faster. More important for this example, when $\alpha = 20$ and $\beta \leq \alpha - 2$, the run time of FBP, SP and OMP are very close. In case $\alpha = 20$ and $\beta = 17$, the speed of FBP and OMP are almost the same, while the reconstruction performance of FBP is significantly better than the other algorithms involved. Note that the speed of FBP can be improved by removing the orthogonal projection after the backward step, at the expense of a slight degradation in the recovery performance.

Finally, we observe that OMP performs better than SP in this example. It yields both higher exact recovery rate and lower ANMSE than SP does. This is due to the chosen OMP termination criterion $\|\mathbf{r}\|_2 \leq \varepsilon \|\mathbf{y}\|_2$. As discussed in Section 2, such a termination criterion provides better recovery results than the OMP scheme that runs for exactly K iterations. Moreover, an estimate of K is not required anymore. A comparison of the OMP recovery performance with the two termination criteria can be found in [18].

4.2. Phase Transitions

Phase transitions are important for empirical evaluation of CS recovery algorithms over a wide range of sparsity levels and

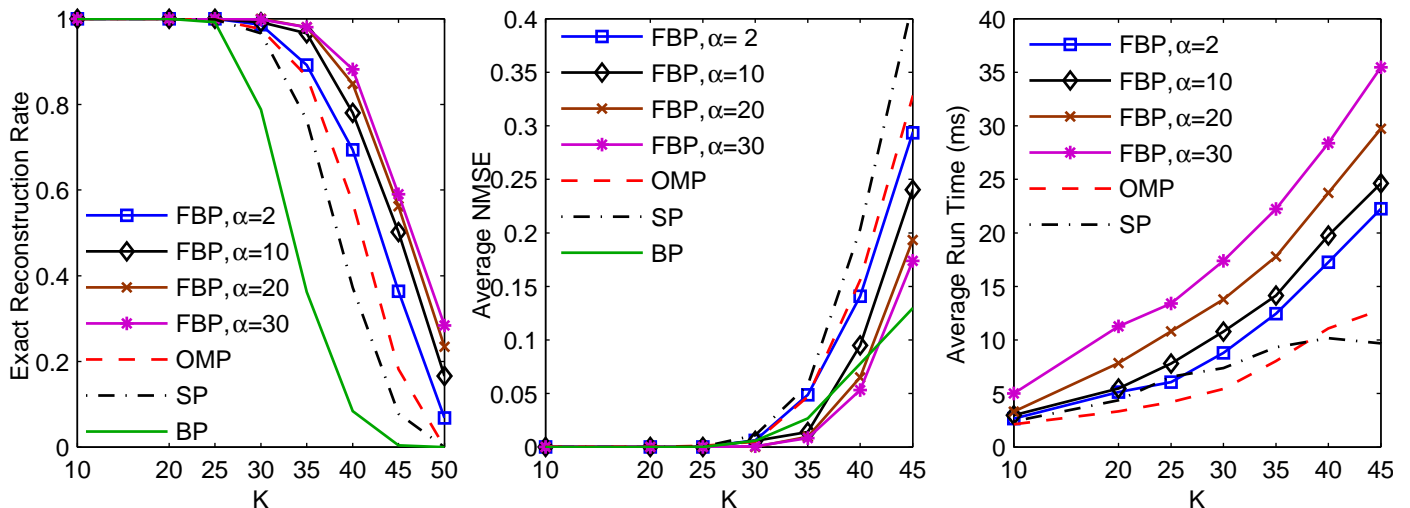


Figure 1: Reconstruction results over sparsity for Gaussian sparse vectors. For FBP, $\beta = \alpha - 1$.

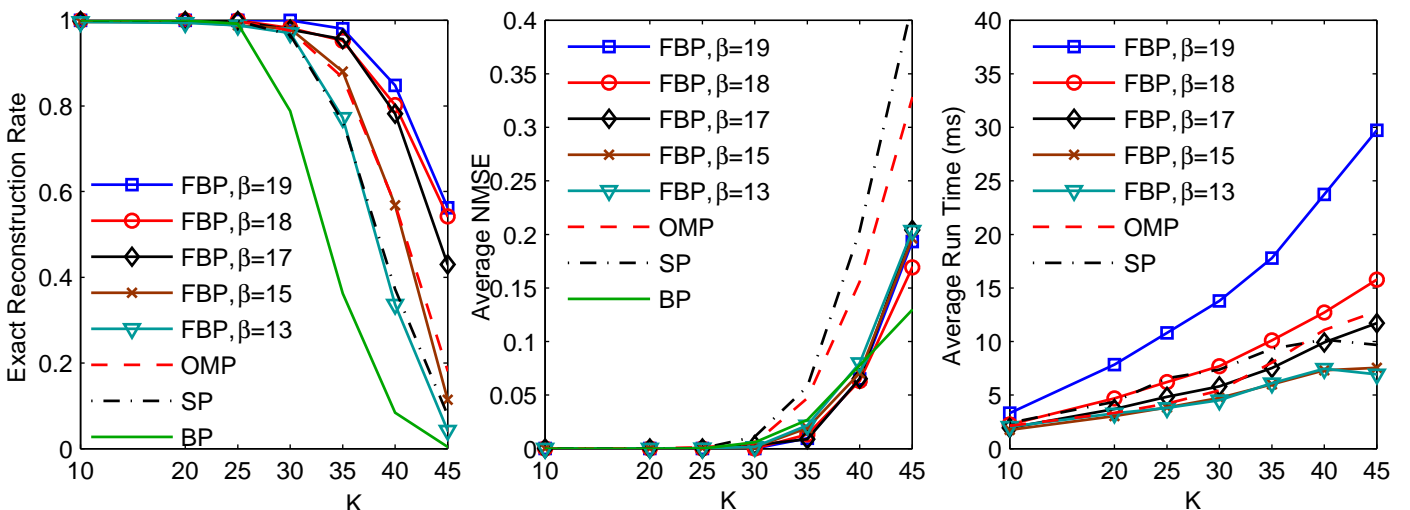


Figure 2: Reconstruction results over sparsity for Gaussian sparse vectors. For FBP, $\alpha = 20$.

observation lengths. These simulations involve three different nonzero element distributions. First one of them is the uniform sparse signals where the nonzero elements are distributed uniformly in $[-1, 1]$. The second type is the Gaussian sparse signals investigated above. The last ensemble involved is the Constant Amplitude Random Sign (CARS) sparse signals (following the naming in [16]) where nonzero elements have constant magnitude 1 with random signs. Below, we first depict phase transitions of FBP with different α and β choices for uniform sparse signals in order to investigate optimality of these over the observation length. These simulations give us a feeling about how to choose FBP step size in relation to M and N . Next, we compare FBP with a fixed setting to BP, OMP and SP for all three test sets.

To explain how we obtain the phase transitions, let's first define normalized measures for observation length and sparsity

level: $\lambda = M/N$ and $\rho = K/M$. To obtain the phase transition curves, we keep the signal length fixed at $N = 250$, and alter M and K to sample the $\{\lambda, \rho\}$ space for $\lambda \in [0.1, 0.9]$ and $\rho \in (0, 1]$. For each $\{\lambda, \rho\}$ tuple, we randomly generate 200 sparse instances and run FBP, OMP, BP and SP algorithms for recovery. For each test example, we employ an individual Gaussian observation matrix as above. We set, $\varepsilon = 10^{-6}$ and $K_{\max} = M$. Specifying the exact recovery condition as $\|\mathbf{x} - \hat{\mathbf{x}}\|_2 \leq 10^{-2} \|\mathbf{x}\|_2$, exact recovery rate is obtained for each $\{\lambda, \rho\}$ tuple and each algorithm. The phase transitions are then obtained using the methodology described in [16]. That is, for each λ , we employ a generalized linear model with logistic link to describe the exact recovery curve over ρ , and then find the ρ value for 50% exact recovery probability.

Phase transitions provide us important means for finding an empirical way of choosing α and β . As discussed in [16], the

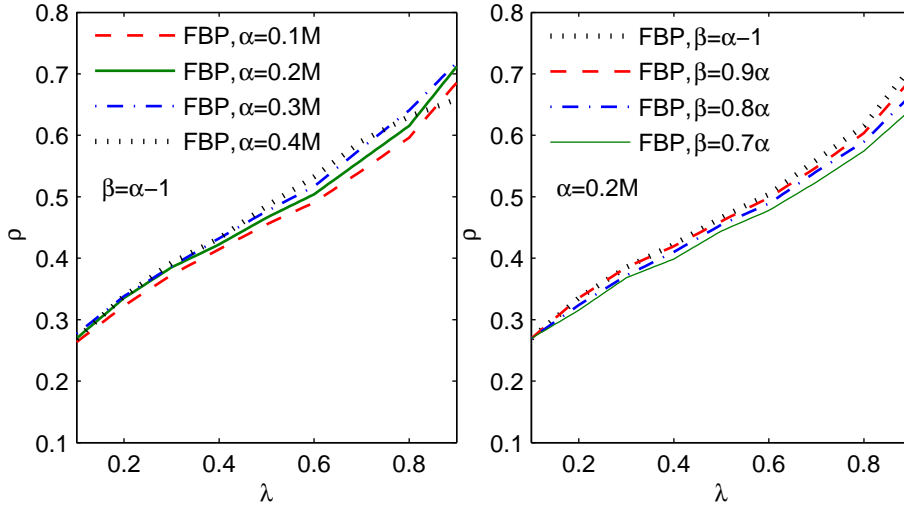


Figure 3: Phase transition of FBP with different forward and backward step sizes for uniform sparse signals.

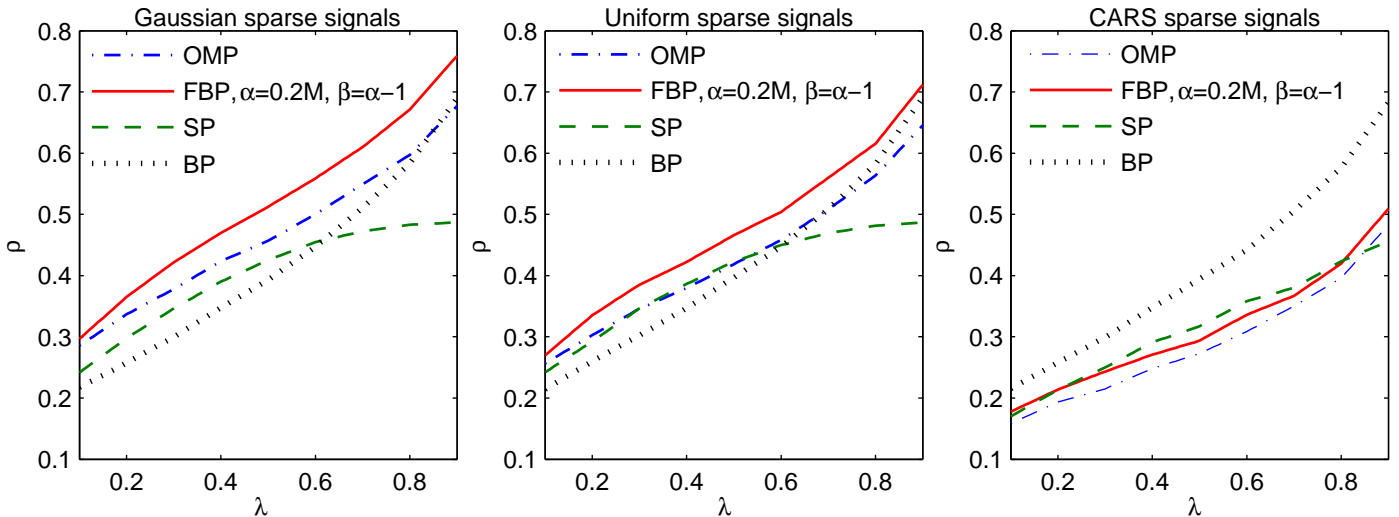


Figure 4: Phase transitions of FBP, BP, SP and OMP for Gaussian, uniform and CARS sparse signals.

phase transition is mostly a function of the λ . Moreover, the transition region turns out to be narrower with increasing λ . These are also supported by some other work in the literature, [19, 20, 21, 22]. Hence, in order to find an optimal set of step sizes for FBP, we need to have a look at the phase transitions using different α and β parameters. Intuitively, α and β should not be fixed but proportional to M . Trying to find fixed α and β values is subject to fail mainly for very low or very high λ values. In other words, it would not be possible an optimal single set $\{\alpha, \beta\}$ for the whole λ range. Hence, we suggest selecting α proportional to M , and β proportional to α . In order to evaluate these, we run two distinct sets of simulations: First, we vary α between $0.1M$ and $0.4M$, while $\beta = \alpha - 1$. Then we fix alpha as $0.2M$ and vary β between 0.9α and 0.7α in order to see how fast the performance degrades with β . The corresponding phase transitions are depicted in Fig. 3.

On the left-side of Fig. 3, we observe that phase transi-

tions are stably improved with α until $\alpha = 0.3M$. Choosing $\alpha = 0.4M$, in contrast, improves the phase transition for the mid- λ region, while the results become worse for low and high λ values. We do not increment α further, however note that doing so would narrow the mid- λ range where recovery is slightly improved, and widen the low and high λ regions where the performance is degraded. Hence, we suggest using $\alpha = 0.3M$ for a globally optimum FBP scheme, while this may be increased if the recovery problem is in the mid- λ region. Note however that the complexity of FBP increases with α , and selecting $\alpha = 0.2M$ may already lead to better phase transition than OMP, BP and SP as demonstrated below.

The graph on the right side of Fig. 3 depicts the phase transitions for different β/α ratios. It is obvious that recovery accuracy degrades with decreasing β , however we are interested in observing how fast this occurs. The results state that the decrease is slight for low λ range. This degradation increases

slightly with λ . The phase transitions for other algorithms are not plotted on this figure, but are available below. In comparison to these, even FBP with β between 0.7α and 0.8α provides a better phase transition curve on general, while BP can do slightly better than this only for λ around $0.8-0.9$. Note that β/α ratio commands the increment in the support per iteration. Reducing this ratio decreases the number of FBP iterations and hence the total run time of FBP. Therefore, the results tell us that it is possible to reduce the complexity of FBP until β is around 0.7 to 0.8 times α , while the phase transition curve is still better than BP, SP and OMP.

Fig. 4 compares the phase transition curve of FBP to those of OMP, BP and SP for Gaussian, uniform and CARS sparse signals, where FBP step sizes are fixed as $\alpha = 0.2M$ and $\beta = \alpha - 1$. For Gaussian and uniform distributions, FBP outperforms the other algorithms, while for the CARS case BP is better than FBP, and the other greedy algorithms. As a consequence of its strong theoretical guarantees and convex structure, the phase transition of BP is robust to the coefficient distribution. Note also that these empirical BP curves are very close to their theoretical counterpart though we do not explicitly plot the theoretical one. SP, FBP and OMP performances degrade for the CARS case, while FBP and OMP curves show the highest variation among different distributions. We observe that when the nonzero values cover a wide range, as for the Gaussian distribution, the performances of FBP and OMP are boosted. On the other hand, nonzero values of equal magnitudes are the most challenging case for these. These observations indicate that these algorithms are more effective when the nonzero elements span a wide range of magnitudes and when this range gets wide enough, even OMP can possess better phase transition than BP.

4.3. Recovery from Noisy Observations

Next, we simulate recovery of sparse signals from noise-contaminated observations. For this purpose, the noisy observation vectors are obtained via contamination by white Gaussian noise at signal-to-noise ratios (SNR) varying from 5 to 40 dB. In this simulation, FBP is run with $\alpha = 20$ and $\beta = 17$, as we have seen above that OMP and FBP require similar run times for this choice. ε is selected with respect to the noise level, such that the remaining residual power is equal to the noise power. The simulation is repeated for 500 Gaussian and 500 uniform sparse signals, where $N = 256$ and $M = 100$. For each test example, we employ an individual Gaussian observation matrix. The sparsity levels are selected as $K = 30$ and $K = 25$ for the Gaussian and uniform sparse signals, respectively. K_{max} is 55 as in the first set of simulations. Fig. 5 depicts the recovery error for noisy Gaussian and uniform sparse signals, while the run times are compared in Fig. 6. Note that we express the recovery error in the decibel (dB) scale, calling it the distortion ratio, in order to make it better comparable with SNR. Clearly, FBP yields the most accurate recovery for both distributions, while BP can do slightly better than FBP only when SNR is 5 dB. The run times reveal that FBP is not only the most accurate algorithm in this example, but is also as fast as OMP with $\alpha = 20$ and $\beta = 17$. Note that, increasing β beyond 17 would improve

FBP recovery, while the algorithm would require a longer run time.

4.4. Demonstration on a Sparse Image

In order to evaluate FBP recovery performance in a more realistic case, we demonstrate recovery of the 512×512 image "bridge". The recovery is performed using 8×8 blocks. The aim for such processing is breaking the recovery problem into a number of smaller, and hence simpler, problems. The image "bridge" is first preprocessed such that each 8×8 block is K -sparse in the 2D Haar Wavelet basis, Ψ , where $K = 12$, i.e. for each block only the $K = 12$ largest magnitude wavelet coefficients are kept. Note that, in this case the signal is not itself sparse, but has a sparse representation in a basis Ψ . Hence, the reconstruction dictionary becomes the holographic basis $\mathbf{V} = \Phi\Psi$. From each block, $M = 32$ observations are taken, where the entries of Φ are randomly drawn from the Gaussian distribution with mean 0 and standard deviation $1/N$. The parameters are selected as $K_{max} = 20$ and $\varepsilon = 9 \times 10^{-7}$. Two set of FBP parameters are tested, $\alpha = 10, \beta = 7$ and $\alpha = 10, \beta = 9$.

Fig. 7 shows the preprocessed image "bridge" on the upper left. On the upper right is the BP recovery. FBP recovery with $\alpha = 10, \beta = 7$ can be found on lower left, and FBP recovery with $\alpha = 10, \beta = 9$ is next to it. In this example, BP provides a Peak Signal-to-Noise Ratio (PSNR) value of 29.9 dB, while the much simpler FBP improves the recovery PSNR up to 32.5 dB. A careful investigation of the recovered images shows that FBP is able to improve the recovery at detailed regions and boundaries. This example demonstrates that the simpler FBP algorithm is able to perform more accurate and faster recovery of a signal with realistic nonzero coefficient distribution than the much more sophisticated ℓ_1 norm minimization approach.

5. Summary

This manuscript proposes the forward-backward pursuit algorithm for CS recovery of sparse signals. FBP, which incorporates iterative forward and backward steps, falls into the category of TST algorithms [16]. The forward step enlarges the support estimate by α atoms, while the backward step removes $\beta < \alpha$ atoms from it. Hence, this two-stage scheme iteratively expands the support estimate for the sparse signal, without requiring K a priori, as SP or CoSaMP do. In comparison to MP type algorithms, FBP provides a backward step for removing possibly misidentified atoms from the solution at each iteration.

FBP recovery performance is demonstrated in Section 5 in comparison to OMP, SP and BP algorithms. The simulations contain recovery of sparse signals with different distributions of the nonzero elements, recovery from noisy observations in addition to the demonstration of the algorithm on a sparse image. The results indicate that except for sparse signals with constant amplitude (the CARS ensemble), FBP can provide better exact recovery rates than OMP, BP and SP. We observe that $\alpha = 0.3M$ and $\beta = \alpha - 1$ lead to near-optimum FBP performance, while these can be decreased in order to speed up the algorithm with a slight sacrifice of the recovery performance. In case of CARS

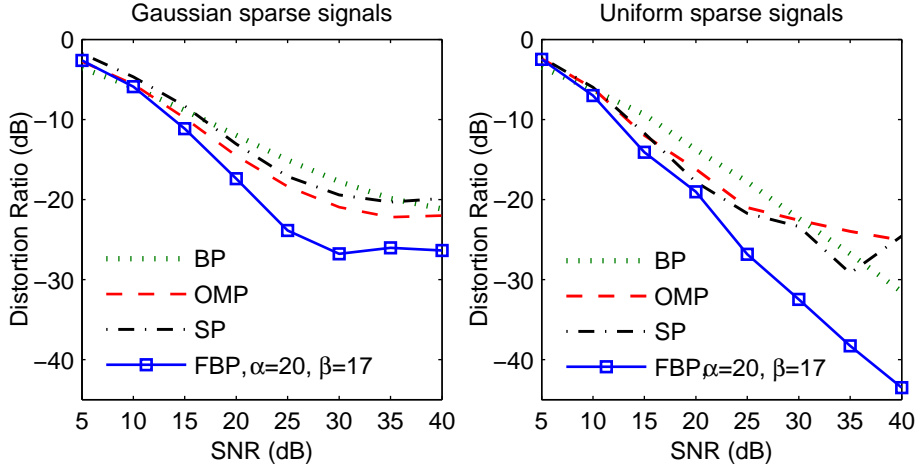


Figure 5: Average recovery distortion over SNR in case of noise contaminated observations. For FBP, $\alpha = 20$ and $\beta = 17$. $K = 30$ and $K = 25$ for the Gaussian and uniform sparse signals, respectively.

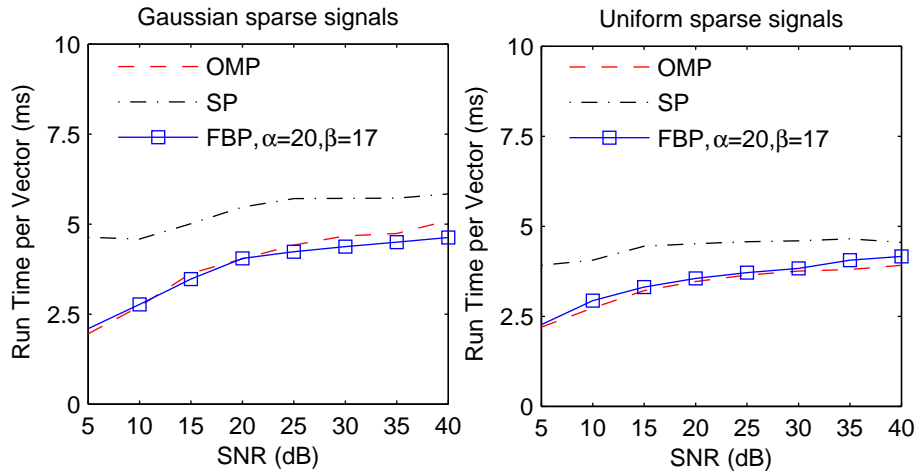


Figure 6: Average run time per test sample in case of noise contaminated observations. For FBP, $\alpha = 20$ and $\beta = 17$. $K = 30$ and $K = 25$ for the Gaussian and uniform sparse signals, respectively.

sparse signals, where the ℓ_0 and ℓ_1 norms are equal, BP turns out to be the most accurate algorithm, outperforming greedy pursuits. Noisy recovery examples state that FBP is robust to observation noise, and provides more accurate recovery under noise than OMP, BP and SP for Gaussian and uniform sparse signals. Finally, demonstration of FBP on a sparse image indicates recovery abilities of the algorithm for sparse signals with realistic nonzero element distributions. We observe that FBP recovery of this sparse image is better than the BP recovery.

Finally, in order to avoid any misinterpretation, we would like to note that our findings do not contradict with the results of Maleki and Donoho in [16], especially in terms of OMP performance. First, we run OMP until the residual power is small enough, i.e. $\|\mathbf{r}\|_2 \leq \epsilon \|\mathbf{y}\|_2$, by which OMP performance is significantly improved over going exactly for K iterations as in [16]. Second, we run the simulations for different nonzero element distributions than in [16]. The results in [16] indicate that

SP is the optimal TST scheme for the CARS ensemble. Our results for the CARS case are parallel to this: SP performs better than FBP and OMP in the CARS scenario, where BP is the best performer. However, [16] does not contain adequate analysis for other types of distributions. Our results show that FBP provides better recovery than SP and BP when the magnitudes of nonzero elements are not comparable. We observe that the FBP performance gets even better when the magnitudes of nonzero elements start spanning a wider range, as for the Gaussian distribution. Even OMP recovery turns out to be better than SP in simulations with Gaussian sparse signals. These indicate that SP is not necessarily the optimum TST scheme for all nonzero element distributions. From a global perspective, CARS sparse signals are the most difficult case for greedy algorithms, and hence the corresponding recovery results can be taken as the worst case performance for greedy algorithms. Therefore, as pronounced in [16], SP has the best worst-case performance

Test image 'bridge'



BP (PSNR = 29.9 dB)



FBP, $\alpha=10$, $\beta=7$ (PSNR = 31.5 dB)



FBP, $\alpha=10$, $\beta=9$ (PSNR = 32.5 dB)



Figure 7: Recovery of the image "bridge" using BP and FBP. BP recovery yields 29.9 dB PSNR, while FBP provides 31.5 dB PSNR for $\alpha = 10$, $\beta = 7$ and 32.5 dB PSNR for $\alpha = 10$, $\beta = 9$.

among TST schemes, while it is outperformed by FBP when the nonzero elements do not have comparable amplitudes anymore. In addition, we think that only a small portion of the real world problems can be represented with constant ampli-

tude sparse signals. Moreover, for most of the problems, it is already known if the signals of interest have comparable magnitudes or not. Hence, the authors of this paper believe that the performance of algorithms for other distributions should be

given more credit. Consequently, FBP is a promising algorithm for signal recovery from compressed measurements.

References

- [1] J. A. Tropp, S. J. Wright, Computational methods for sparse solution of linear inverse problems, *Proc. IEEE* 98 (2010) 948–958.
- [2] E. Candès, T. Tao, Decoding by linear programming, *IEEE Trans. Inf. Theory* 51 (2005) 4203–4215.
- [3] E. Candès, T. Tao, Near-optimal signal recovery from random projections: universal encoding strategies?, *IEEE Trans. Inf. Theory* 52 (2006) 5406–5425.
- [4] E. Candès, The restricted isometry property and its implications for compressed sensing, *Comptes Rendus Mathématique* 346 (2008) 589–592.
- [5] E. Candès, J. Romberg, Practical signal recovery from random projections, in: *Proc. SPIE Computational Imaging*, volume 5674, pp. 76–86.
- [6] D. L. Donoho, Compressed sensing, *IEEE Trans. Inf. Theory* 52 (2006) 1289–1306.
- [7] D. L. Donoho, M. Elad, Optimally sparse representation in general (nonorthogonal) dictionaries via ℓ_1 minimization, in: *Proc. Natl. Acad. Sci.*, volume 100, Los Alamitos, CA, p. 21972202.
- [8] S. Chen, D. L. Donoho, M. Saunders, Atomic decomposition by basis pursuit, *SIAM J. on Sci. Comp.* 20 (1998) 33–61.
- [9] S.-J. Kim, K. Koh, M. Lustig, S. Boyd, D. Gorinevsky, An interior point method for large-scale ℓ_1 -regularized least squares, *IEEE Journal on Selected Topics in Signal Processing* 1 (2007) 606–617.
- [10] S. Mallat, Z. Zhang, Matching pursuit in a time-frequency dictionary, *IEEE Trans. Signal Process.* 41 (1993) 3397–3415.
- [11] Y. C. Pati, R. Rezaifar, P. S. Krishnaprasad, Orthogonal matching pursuit: Recursive function approximation with applications to wavelet decomposition, in: *Proc. 27th Asilomar Conference on Signals, Systems and Computers*, volume 1, Los Alamitos, CA, pp. 40–44.
- [12] D. Needell, J. A. Tropp, CoSaMP: Iterative signal recovery from incomplete and inaccurate samples, *Appl. Comp. Harmonic Anal.* 26 (2008) 301–321.
- [13] W. Dai, O. Milenkovic, Subspace pursuit for compressive sensing signal reconstruction, *IEEE Trans. Inf. Theory* 55 (2009) 2230–2249.
- [14] T. Blumensath, M. Davies, Iterative thresholding for sparse approximations, *J. Fourier Anal. Appl.* 14 (2008) 629–654.
- [15] T. Blumensath, M. Davies, Iterative hard thresholding for compressed sensing, *Appl. Comp. Harmonic Anal.* 27 (2009) 265–274.
- [16] A. Maleki, D. Donoho, Optimally tuned iterative reconstruction algorithms for compressed sensing, *Selected Topics in Signal Processing*, *IEEE Journal of* 4 (2010) 330–341.
- [17] T. Zhang, Adaptive forward-backward greedy algorithm for learning sparse representations, *IEEE Trans. Inf. Theory* 57 (2011) 4689–4708.
- [18] N. B. Karahanoglu, H. Erdogan, A comparison of termination criteria for A*OMP, in: *European Signal Processing Conference*, Bucharest, Romania.
- [19] R. Berinde, A. C. Gilbert, P. Indyk, H. Karloff, M. J. Strauss, Combining geometry with combinatorics: A unified approach to sparse signal recovery, in: *Proc Allerton Conf. Commun. Control, Comput.*
- [20] D. L. Donoho, Y. Tsaig, Fast solution of ℓ_1 -norm minimization problems when the solution may be sparse, *IEEE Trans. Inf. Theory* 54 (2008) 4789–4812.
- [21] D. Donoho, Y. Tsaig, I. Drori, J.-L. Starck, Sparse solution of underdetermined systems of linear equations by stagewise orthogonal matching pursuit, *IEEE Trans. Inf. Theory* 58 (2012) 1094–1121.
- [22] D. L. Donoho, J. Tanner, Counting the faces of randomly-projected hypercubes and orthants, with applications, *Discrete Comput. Geom.* 43 (2010) 522–541.